Statistical Distribution of Intensities Reflected from Disordered Media

A. García-Martín, T. López-Ciudad, J.J. Sáenz

Departamento de Física de la Materia Condensada and Instituto de Ciencia de Materiales "Nicolás Cabrera", Universidad Autónoma de Madrid, E-28049 Madrid, Spain.

M. Nieto-Vesperinas

Instituto de Ciencia de Materiales de Madrid. Consejo Superior de Investigaciones Científicas, Campus de Cantoblanco, E-28049 Madrid, Spain.
(12 March 1998)

A theoretical analysis of the statistical distributions of the reflected intensities from random media is presented. We use random matrix theory to analytically deduce the probability densities in the localization regime. Numerical calculations of the coupling to backward modes in surface corrugated waveguides are also put forward for comparison. Interestingly, the speckle distributions are found to be independent of the transport regime. Despite the scattering being highly non-isotropic, the predicted probability densities reproduce accurately the numerical results.

PACS numbers: 42.25.Bs, 41.20.Jb, 5.45.+b, 84.40.Az

The scattering of both classical and quantum waves from random media has long been a subject of interest [1]. Interesting multiple scattering effects like the enhanced backscattering (EB) [2,3] and intensity correlations in transmitted and reflected waves [4–6] have extensively been analyzed. Recently much attention has been focused on this subject in connection with the probability distributions of the different transmittances in disordered waveguides [7–11]. Rayleigh and Gaussian statistics with anomalous tails in the diffusive regime, observed experimentally [9], were analytically deduced within the random matrix theory (RMT) framework [7,12]. A strong dependence on the length L of the disordered region was expected from numerical simulations of waveguides with volume disorder [13]. Recent results [8], also based on RMT, have shown how the Rayleigh and Gaussian distributions evolve into the same lognormal distribution as L increases beyond the localization length ξ. The same behavior has been found in simulations of surface corrugated waveguides [11]. However, in contrast with the transmission case, the probability distributions of reflected intensities have not been discussed in detail previously. It is the purpose of this work to put forward a comprehensive picture of the statistics of reflected waves from a disordered waveguide based on analytical as well as on numerical calculations.

In order to discuss some general properties of the backward scattering, random matrix theory provides a useful macroscopic approach since it does not depend on the specific details of the scattering processes. We will make use of RMT results to analytically deduce the probability density of the reflected *speckle pattern* in a N-mode waveguide in the localized regime. As expected from the central limit theorem, in the limit of large N, the speckle distribution follows a negative exponential law (Rayleigh statistics). As a consequence of enhanced coherent backscattering effects (i.e. time-reversal invariance [6]), as N decreases, this Rayleigh law evolves into two different distributions depending on the backward scattering directions. The numerical calculations of the speckle statistics for a corrugated waveguide show a remarkable agreement with these analytical results all the way from the diffusive through the strong localized regime. Although the analytical results are formally deduced in localization, this agreement indicates that, in contrast with transmission, *the reflected speckle distributions are independent of the transport regime.*

Our theoretical approach is based on the properties of the scattering matrix S of a waveguide with a central region containig the random medium (whose disorder can be indistinctly either in volume or in the walls) (see Fig.1). Outside this region, the transverse confinement in the waveguide defines N propagating modes or channels [14]. The wave transport can be described in terms of the scattering matrix S:

$$\begin{pmatrix} r & \tilde{t} \\ t & \tilde{r} \end{pmatrix} , \qquad (1)$$

where r, $\tilde{t}$, t, $\tilde{r}$, are square matrices whose dimension is given by the total number of channels N. The matrix elements r_{ij} and t_{im} are the reflected and transmitted amplitudes into the channels j and m, respectively,

when there is a unit flux in the channel i incident from the left; $\tilde{r}_{nm}$ and $\tilde{t}_{nj}$ have the same meaning but the incoming channel is incident from the right. In terms of these elements, the transport coefficients $R_{ij} = |r_{ij}|^2$ and $T_{im} = |t_{im}|^2$ measure the reflected and transmitted speckle patterns respectively, being $R_i = \sum_j R_{ij}$ and $T_i = \sum_m T_{im}$ the total reflection and transmission for the incoming mode i.

The study of the probability densities of the reflected intensities $P(R_{ij})$ is much simpler in the strong localization regime where the transmission amplitudes vanish. The matrix S is then reduced to the two square blocks r and $\tilde{r}$. Since we are interested in a statistical approach, given our limited knowledge of the microscopic coupling between channels, the natural choice of the statistical ensemble is that which maximize the information entropy subject to the known constrains [*flux conservation* (S unitary) and *time-reversal invariance* (S symmetric)]. In the RMT context, this leads to the circular orthogonal ensemble (COE, $\beta = 1$), i.e. the phases of the elements of the reflection blocks are as random as possible while their moduli are constrained by the conditions of unitarity and symmetry. In the absence of time reversal invariance, the matrix S loses its symmetry and the appropriate statistical ensemble is then the circular unitary ensemble (CUE, $\beta = 2$).

Following general formulas for the distribution of matrix elements in the circular ensembles derived by Pereyra and Mello [15], we can compute the distribution of the reflected speckle pattern $P(R_{ij})$. Due to the underlying *isotropy* condition [5,12] the RMT results are mode independent except for the backscattering into the same channel:

$$P(R_{ii}, \beta = 1) = \left(\frac{1}{\langle R_{ii} \rangle} - 1 \right) (1 - R_{ii})^{1/\langle R_{ii} \rangle - 2} , \quad (2)$$

and

$$P(R_{ij}, \beta = 1) = \left(\frac{1}{2\langle R_{ij} \rangle} - 1 \right) (1 - R_{ij})^{1/\langle R_{ij} \rangle - 3}$$
$$\times \, {}_2F_1\left(\frac{1}{2\langle R_{ij} \rangle} - 1, 1; \frac{1}{\langle R_{ij} \rangle} - 2, 1 - R_{ij} \right) , (i \neq j) , \quad (3)$$

where ${}_2F_1$ is the hypergeometric function and the mean values $\langle R_{ij} \rangle$ are given by [5,6]:

$$\langle R_{ij} \rangle = \frac{1 + \delta_{ij}\delta_{\beta 1}}{N + \delta_{\beta 1}} . \quad (4)$$

Although recent numerical calculations [11,16,17] show that the different channels are not equivalent, as we will see, the actual statistical distributions can still be described by the general RMT results. The key point will be to consider the distributions as functions of the mean values rather than in terms of the number of channels.

In Figs. 2 and 3 we have plotted Eqs. (2) and (3) for a set of values of $\langle R_{ii} \rangle$ and $\langle R_{ij} \rangle$, respectively (thick solid

and broken lines), together with numerical results for a surface corrugated waveguide (see the details below). To this end, $\langle R_{ij} \rangle$ always involves $i \neq j$. In the limit of N large , (both $\langle R_{ii} \rangle$ and $\langle R_{ij} \rangle \ll 1$), both distributions (2) and (3) evolve into a Rayleigh law. Coherent backscattering effects manifest themselves in the distributions for small N which dramatically depend on whether $i = j$, or $i \neq j$. This is illustrated in the analysis of the case $N = 2$ ($\langle R_{ii} \rangle = 2/3$ and $\langle R_{ij} \rangle = 1/3$) where the probabilities for $i = j$ and for $i \neq j$ are quite different (see inset in Fig. 3):

$$P(R_{ii}, \beta = 1) = \frac{1}{2\sqrt{1 - R_{ii}}} , \quad (5)$$

and

$$P(R_{ij}, \beta = 1) = \frac{1}{2\sqrt{R_{ij}}} , (i \neq j) . \quad (6)$$

When time reversal symmetry is removed, there is no longer difference between $P(R_{ij})$ and $P(R_{ii})$, and hence there is a unique intensity distribution. Interestingly, in terms of the averages the statistical law coincides with that obtained for R_{ii} in the case of $\beta = 1$, i.e.

$$P(R_{ij}, \beta = 2) = P(R_{ii}, \beta = 2) = P(R_{ii}, \beta = 1) . \quad (7)$$

This means that the *statistical law* that governs the backscattered intensities R_{ii} does not depend on the time reversal symmetry conditions, as long as they are expressed in terms of the mean value.

It is worth noticing, that for a chaotic cavity [18], Eqs. 2 and 3 are exact results tor the reflected intensities for any N. In this case, $\langle R_{ij} \rangle = (1 + \delta_{ij}\delta_{\beta 1})(2N + \delta_{\beta 1})^{-1}$. Again, in terms of the mean values, the statistics of reflected waves from a chaotic cavity and from a waveguide in the localization regime are indistinguishable.

Let us now discuss the numerical results for the reflection coefficients in a surface disordered waveguide (see Fig. 1). The corrugated part of the waveguide, of total length L and perfectly reflecting walls, is composed of n slices of length l. The width of each slice has random values uniformly distributed between $W_0 - \delta$ and $W_0 + \delta$ about a mean value W_0. Following previous works, we shall take $W_0/\delta = 7$ and $l/\delta = 3/2$. The main transport properties do not depend on the particular choice of these parameters, however [11,19]. Transmission and reflection coefficients are exactly calculated by solving the 2D wave equation by mode matching at each slice, together with a generalized scattering matrix technique [19–21]. In order to obtain the intensity distributions as well as the mean values for the reflection coefficients, we have performed the calculations over an ensemble of one thousand configurations.

The anisotropy of the scattering process, predicted in Refs. [11,16,17], is specially relevant when the EB factor η_i, defined as

$$\eta_i = (N-1)\frac{\langle R_{ii}\rangle}{\langle R_i\rangle - \langle R_{ii}\rangle} \ , \tag{8}$$

is addressed. This EB factor is very sensitive to the changes in the mean values, and so it is specially affected by changes in the incident wavelength. In Fig. 4b we show the behavior of η as a function of the wavelength, for a length of the corrugated part such that the system is always in the localization regime. The behavior of the "external" modes (defined as those propagating modes with either the smallest or the largest transversal momentum) is quite different to that of the "central" ones. The lowest mode (i.e. that with the smallest transversal momentum) has a marked oscillatory value of η, showing peaks at the onset of each new propagating mode in the waveguide. For the rest of the modes, except for small oscillations, η evolve from a high value just at the onset of propagation, to the expected factor of 2. This oscillating behavior is closely related to that observed in the localization length ξ shown in Fig. 4a, (see also Ref. [19]).

The numerical probability densities have been calculated in the range of wavelengths shown in Fig. 4, for different length values including both the diffusive ($\xi/N \lesssim L \lesssim \xi$) and localized ($L \gtrsim \xi$) regimes. The histograms in Fig. 2 and 3 (thin solid lines) show the intensity distributions numerically obtained for different averages of either $\langle R_{ii}\rangle$ or $\langle R_{ij}\rangle$. Distributions corresponding to different number of propagating modes and different transport regime, but having the same average of the reflection coefficient, are indistinguishable. Despite being the scattering highly non-isotropic, it is remarkable that both numerical and analytical results coincide with each other, without any adjustable parameter. This indicates that, while the average values depend on the specific system under consideration, the fluctuations, which are characteristics of disordered systems, are fully represented by the probability density *as a funtion of the mean values*, and have general properties that are well described by RMT.

In summary, we have derived the general statistical properties of the reflected intensities from a random medium in the localization regime, based on RMT. Comparisons have been made by numerically analizing the coupling to backward modes in surface corrugated waveguides. The enhanced backscattering factor can be much larger than that predicted by RMT, and oscillates versus the wavelength following the oscillating behavior observed for the localization length. We show, however, that in spite of the anisotropy of the interactions, the numerical statistical distributions accurately follow the RMT predictions, independently of the transport regime. This indicates that the statistical distributions do not depend on the details of the scattering processes. They should then be observable in different systems under rather general disorder conditions.

[1] P. Sheng ed. *"Scattering and localization of classical waves in random media"*, (World Sci., Singapore, 1990); M. Nieto-Vesperinas and J.C. Dainty eds., *"Scattering in Volumes and Surfaces"*, (North Holland, Amsterdam, 1990); C.W.J Beenakker and H. van Houten, in *Solid State Physics: Advances in Research and Applications*, H. Ehrenreich and D. Turnbull (Academic, San Diego, 1991),Vol. 44; P. Sheng *"Introduction to Wave Scattering, Localization and Mesoscopic Phenomena"*, Academic Press, N.Y. (1995).

[2] Y. Kuga and J. Ishimaru, J. Opt. Soc. Am. A, **1**, 831 (1984); M.P. van Albada and A. Lagendijk, Phys. Rev. Lett. **55**, 2692 (1985); P.E. Wolf and G. Maret, *ibid* **55**, 2696 (1985); E. Akkermans, P.E. Wolf and R. Maynard, *ibid* **56**, 1471 (1986); M. Kaveh, M. Rosenbluh, M. Edrei and I. Freud, *ibid* **57**, 2949 (1986).

[3] A.R. McGurn, A. Maradudin and V. Celli, Phys. Rev. B **31**, 4866 (1985); K.A. O'Donnell and E.R. Mendez, J. Opt. Soc. Am. A **4**, 1194 (1987); M. Nieto-Vesperinas and J.M. Soto-Crespo, Opt. Lett. **12**, 979 (1987).

[4] E. Wolf, Phys. Rev. Lett. **56**, 1370 (1986); B. Shapiro, *ibid* **57** 2168 (1986); M. Stephen and G. Cwilich, *ibid* **59**, 285 (1987); S. Feng, C. Kane, P.A. Lee and A.D. Stone, *ibid* **61**, 834 (1988); I. Freund, M. Rosenbluh and S. Feng, *ibid* **61**, 2328 (1988); N. García and A.Z. Genack, *ibid* **63** 1678 (1989); R. Berkovits, M. Kaveh and S. Feng, Phys. Rev. B **40**, 737 (1989); M. P. van Albada, J.F. de Boer and A. Lagendijk, Phys. Rev. Lett. **64** 2787 (1990).

[5] P.A. Mello, E. Akkermans and B. Shapiro, Phys. Rev. Lett. **61**, 459 (1988).

[6] E. Bascones, M.J. Calderón, D. Castello, T. López-Ciudad and J.J. Sáenz, Phys. Rev. B **55**, R11911 (1997).

[7] Th. M. Nieuwenhuizen and M.C.W. van Rossum, Phys. Rev. Lett. **74**, 2674 (1995); E. Kogan and M. Kaveh, Phys. Rev. B **52**, R3813 (1995).

[8] S.A. van Lagen, P.W. Brouwer and C.W.J. Beenakker, Phys. Rev. E **53**, R1344 (1996).

[9] A.Z. Genack and N. Garcia, Europhys. Lett. **21**, 753 (1993); J.F. de Boer, M.C.W. van Rossum, M.P. van Albada, Th. M. Nieuwenhuizen and A. Lagendijk, Phys. Rev. Lett. **73** 2567 (1994); M. Stoytchev and A.Z. Genack, *ibid* **79**, 309 (1997).

[10] J.A. Torres and J.J. Sáenz, Phys. Rev. Lett. **77** 2245 (1996);E. Bascones, G. Gómez-Santos and J.J. Sáenz, Phys. Rev. B **57**, 2541 (1998).

[11] A. García-Martín, J.A. Torres, J.J Sáenz and M. Nieto-Vesperinas, Phys. Rev. Lett. **80**, 4165 (1998).

[12] For a review on RMT see C.W.J. Beenakker, Rev. Mod. Phys. **69**, 731 (1997).

[13] I. Edrei, M. Kaveh and B. Shapiro, Phys. Rev. Lett. **62**, 2120 (1989).

[14] In the case of a sample in free space no discrete modes exist. Here, a channel is a solid angle containing one coherence area or - in practical terms - having the size of a speckle spot. The number of channels in this case is given by $N = 2\pi A/\lambda^2$ where A is the cross section of the waveguide or the illuminated area of the sample.

[15] P. Pereyra and P.A. Mello, J. Phys. A **16** 237 (1983).

[16] P. García-Mochales, P.A. Serena, N. García and J.L. Costa-Krämer, Phys. Rev. B **53**,10 268 (1996); P. García-Mochales and P.A. Serena, Phys. Rev. Lett **79**, 2316 (1997).

[17] J.A. Sánchez-Gil, V. Freilikher, I. Yurkevich and A.A. Maradudin, Phys. Rev. Lett. **80**, 948 (1998).

[18] H.U. Baranger and P.A. Mello, Phys. Rev. Lett. **73**, 142 (1994); Phys. Rev. B **54**, R14297 (1996); R.A. Jalabert, J.L. Pichard and C.W.J. Beenakker, Europhys. Lett. **27**, 255 (1994).

[19] A. García-Martín, J.A. Torres, J.J. Sáenz and M. Nieto-Vesperinas, Appl. Phys. Lett, **71**, 1912 (1997).

[20] A. Weisshaar, J. Lary, S. M. Goodnick and V.K. Tripathi, J. Appl. Phys. **70**, 355 (1991)

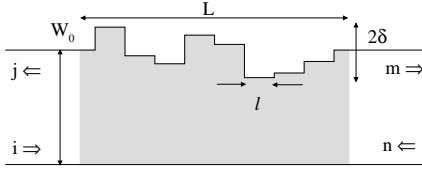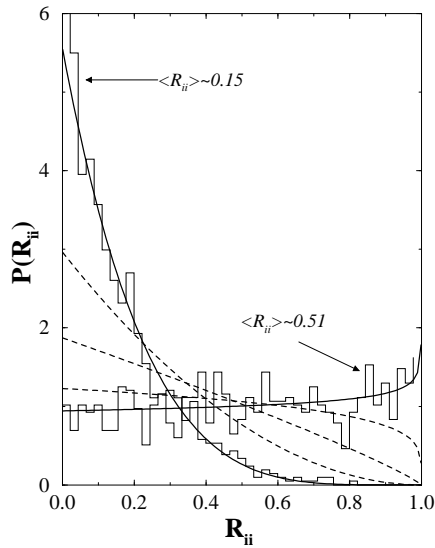[21] J.A. Torres and J.J. Sáenz, unpublished. J.A. Torres, Ph. D. Thesis, Universidad Autónoma de Madrid (1997).

FIG. 2. Distributions of R_{ii} for different values of $\langle R_{ii} \rangle$. Thin solid lines correspond to the numerical calculations for $\langle R_{ii} \rangle \sim 0.15, 0.51$, respectively, whereas thick solid lines are the analytical predictions. Thick broken lines are the analytical results for $\langle R_{ii} \rangle \sim 0.25, 0.35$ and 0.45, respectively.
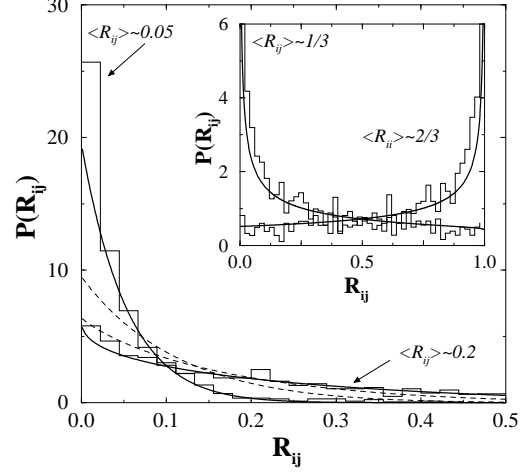

FIG. 3. Distributions of $R_{ij}(i \neq j)$ for different values of $\langle R_{ij} \rangle$. Thick solid lines are the analytical predictions for the same values of the averages, as those indicated for the numerical histograms (thin solid lines) ($\langle R_{ij} \rangle \sim 0.05, 0.2$, respectively). Thick broken lines are the analytical results for $\langle R_{ij} \rangle \sim 0.10$ and 0.15, respectively. Inset: Probability density for $N = 2$: $P(R_{ii})$ ($\langle R_{ii} \rangle = 2/3$), and $P(R_{ij})$ ($\langle R_{ij} \rangle = 1/3$).

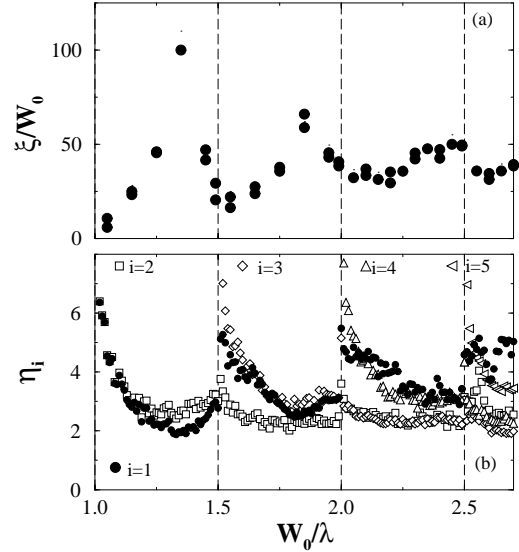FIG. 1. Schematic view of the system under consideration.

FIG. 4. (a) Localization length ξ versus W_0/λ. (b) Enhanced backscattering factor η_i versus W_0/λ. Vertical long-dashed lines are drawn at the onset of a new mode.